Transfer of Solar Irradiance through Cirrus Cloud Layers

KUO-NAN LIOU

Department of Atmospheric Sciences, University of Washington
Seattle, Washington 98195

Reflection, transmission, and absorption of several cirrus cloud layers as functions of the solar zenith angle are obtained in the visible and near infrared of the solar spectrum by simplified radiative transfer calculations. The single-scattering computations for cirrus are carried out on the assumption that they contain randomly oriented long cylinders. The scattering parameters such as the phase function, the single-scattering albedo, and the extinction cross section are formulated and evaluated for incident wavelengths of 0.7, 2, 2.5, and 3 μ. A modified transfer method is developed with an approximation made only in the integral form of the radiative transfer equation. The method, which uses a small amount of computer time, yields an accuracy within 3% in most cases of conservative as well as nonconservative scattering. It is found that at 0.7 μ visible light a typical cirrus with an optical thickness of $\sim$2 shows a local albedo of $\sim$20% for zenith angles up to $\sim$60°. High values of transmission may be anticipated even if large absorption occurs in the clouds.

Considerable interest has been focused on the problem of the influence of cirrus on the atmospheric heat balance and its interfering effects on the sensing of the atmospheric structure from orbiting meteorological satellites. Although measurements of the transmission of cirrus in the thermal infrared have recently been reported by *Fritz and Rao* [1967], *Hall* [1968], *Kuhn and Weickmann* [1969], and *Cox* [1971], it appears that neither experiments nor comprehensive theoretical studies have been undertaken to investigate the transfer of solar irradiance through cirrus cloud layers. Since the sun is the primary thermal source driving our atmosphere, the influence of the large amount of globally distributed cirrus on solar radiation should be carefully examined. This paper derives from a theoretical point of view some radiative properties of cirrus cloud layers.

Cirrus contains predominantly nonspherical hexagonal columns [*Weickmann*, 1949]. The nonsphericity creates a great deal of difficulty in the light-scattering analysis. To tackle the problem theoretically, the assumption is made that the ice crystals in cirrus may be approximated by long circular cylinders that are randomly oriented in space. The physical formulations of the phase function and the scattering cross section for arbitrarily oriented cylinders have been described in a previous paper [*Liou*, 1972*b*]. In addition to these two scattering parameters we have further developed here a traceable theory for obtaining the extinction cross section so as to complete the scattering computations for use in the later transfer program.

A simplified radiative transfer method dealing particularly with flux distribution is developed to evaluate the radiative properties of cirrus cloud layers in the visible and near-infrared wavelengths. Although this method includes the exact contribution by the single scattering, the effects of multiple scattering are approximated by combining the downward and upward streams of radiation. The part of approximation is quite similar to the work previously illustrated by *Shettle and Weinman* [1970] and *McElroy* [1971]. The simplified method, which is practical for application to evaluate radiation field in turbid atmospheres, is named the modified two-stream approximation for radiative transfer (MTSA). Comparisons of the results obtained by MTSA with those of the more exact computations by means of a doubling method [*Irvine*, 1968; *Hansen*, 1969] reveal close agreement in most cases of conservative and nonconservative scattering.

By employing the single-scattering results for the cirrus cloud model in the transfer program described above, radiative properties such as

transmission, reflection, and absorption are obtained as functions of the solar zenith angle as well as the cloud thickness.

SINGLE SCATTERING BY RANDOMLY ORIENTED ICE CYLINDERS

On the basis of the comprehensive observations reported by *Weickmann* [1949], several physical properties of ice crystals in cirrus may be summarized as follows. The shapes of crystals are predominantly hexagonal columns. A typical cirrus particle may be 200 μ in length and 30 μ in width. The averaged particle concentration is ~ 0.5 cm^{-3}. Since it is unlikely that a classical scattering theorem for shapes such as hexagonal columns could be formulated and solved, we assume in this theoretical investigation that crystals in cirrus may be approximated by long circular cylinders randomly oriented in space. On the basis of these assumptions the scattering computations for such hypothetical cirrus models can therefore be carried out.

Light scattering by single long cylinders has been investigated by *Kerker* [1969] and *Liou* [1972*a*]. *Liou* [1972*b*] has further extended the scattering problems to a sample of cylinders with orientations and sizes taken into consideration in which the theoretical formulations for the phase function and the scattering cross section have been described in some detail. However, a more traceable physical development for obtaining the extinction cross section for arbitrarily oriented cylinders has not been given. (And it has not been discussed in the literature elsewhere to my knowledge, though *van de Hulst* [1957] has outlined some general procedures.) Therefore we shall now proceed to develop briefly the theory of extinction for an arbitrarily oriented cylinder, since this quantity is needed in the multiple-scattering computations discussed below.

Theory of extinction. The amplitude of the incident wave for a long cylinder may be written as

$$\psi_0(\alpha) = \exp [i\omega t - ik(x \cos\alpha + z \sin\alpha)] \quad (1)$$

where ω is the circular frequency, k is the wave number, α is the incident angle, x and z are distances along two axes of the rectangular coordinate system, and $i = (-1)^{1/2}$. The amplitude of the scattered wave for large R, which represents the distance of the propagation of the wave, was given by [*Liou*, 1972*a*]

$$\psi(\alpha, \phi) = (2/\pi kR)^{1/2} T(\alpha, \phi) \cdot \exp (i\omega t - ikR - i3\pi/4) \quad (2)$$

where ϕ is an angle indicating the distribution of the scattered energy and $T(\alpha, \phi)$ represents any outgoing cylindrical wave.

We wish to evaluate the combined intensity of the incident and scattered waves at the forward direction ($\phi = 0$) in the far field. We note the following geometrical relationships:

$$\begin{aligned} R &= r \cos\alpha + z \sin\alpha \\ x &= r \cos\phi \\ y &= r \sin\phi \end{aligned} \quad (3)$$

If $\phi \to 0$ and $R \to \infty$, we have

$$r = (x^2 + y^2)^{1/2} \simeq x + (y^2/2R) \quad (4)$$

When the incident and scattered waves are added and terms of the order of $1/R$ higher than $(1/R)^{1/2}$ are neglected, the combined intensity becomes

$$|\psi_0(\alpha) + \psi(\alpha, 0)|^2 \simeq 1 + 2(2/\pi kR)^{1/2} \text{ Re } [T(\alpha, 0)x \cdot \exp (-iky^2/2R - i3\pi/4)] \quad (5)$$

where Re [ ] represents the real part of the argument.

Integrating the combined intensity over the entire cylinder having a width of d and a length of l, we obtain the total power received by the cylinder

$$\int_0^l \int_0^d |\psi_0(\alpha) + \psi(\alpha, 0)|^2 \, dy \, dz = l(d - c_e) \quad (6)$$

where lc_e denotes the amount of the reduction of the incident energy as if an objective whose area was lc_e had been covered up. To obtain the quantity c_e, which may be physically explained as an extinction cross section per unit length, we note the following. In the forward direction $\phi \to 0$, the integration limits of y may theoretically extend to infinity. Thus we obtain the following Fresnel integral:

$$\int_{-\infty}^{+\infty} \exp\left(\frac{-iky^2}{2R}\right) dy = \left(\frac{2\pi R}{k}\right)^{1/2} \exp\left(\frac{-i\pi}{4}\right) \quad (7)$$

Substituting (5) and (7) into (6), we have

$$c_e(\alpha) = (4/k)\ \mathrm{Re}\ [T(\alpha, 0)] \quad (8)$$

The final result for the extinction cross section for an arbitrarily oriented cylinder illuminated by the unpolarized incident wave may be written as

$$c_e(\alpha) = \frac{2}{k}\ \mathrm{Re}\left[b_{01} + a_{02} + 2\sum_{n=1}^{\infty}(b_{n1} + b_{n2} + a_{n1} + a_{n2})\right] \quad (9)$$

where a_n and b_n are scattering coefficients previously derived by *Liou* [1972*a*]. Moreover, considering the problem of orientation, I have also discussed the geometry involved [*Liou*, 1972*b*]. The angles responsible for the orientation in the vertical direction ϵ and the horizontal direction γ are related to the incident angle α as

$$\sin\alpha = \cos\epsilon\cos\gamma \quad (10)$$

Furthermore, it has been shown by *Twersky* [1954] that, if the cylinder has an inclination angle α with the incident ray, a factor of sec α should be taken into account when a sample of cylinders is considered. Hence the average extinction cross section for a sample of randomly oriented long cylinders may be expressed as

$$\langle c_e\rangle = \frac{2}{\pi^2}\int_0^{\pi/2}\int_0^{\pi} c_e(\alpha)\sec\alpha\, d\epsilon\, d\gamma \quad (11)$$

A similar definition can be applied for the averaged scattering cross section $\langle c_s\rangle$. Finally, the single-scattering albedo and the phase function for a sample of randomly oriented long cylinders with the incident wave unpolarized may be written as

$$\tilde{\omega}_0 = \langle c_s\rangle/\langle c_e\rangle \quad (12)$$

and

$$P(\Theta) = \frac{1}{\langle c_s\rangle}\int_0^{\pi/2}\int_0^{\pi} i(\Theta;\gamma,\epsilon)\, d\epsilon\, d\gamma \quad (13)$$

respectively, where i is the intensity coefficient for an incident unpolarized light. For properly presenting graphs in the section the phase functions are all normalized such that when they are integrated over the solid angle they become 1.

Single-scattering computations. On the basis of the reasoning described above, computations of the optical properties of randomly oriented ice cylinders are carried out for the visible and near-infrared wavelengths of 0.7, 2, 2.5, and 3 μ. The refractive indices of ice cylinders at each wavelength are taken from the table by *Irvine and Pollack* [1968] and are shown in Table 1. In the scattering computations for incident wavelengths of 2, 2.5, and 3 μ we use cylinders 200 μ in length and 30 μ in radius, whereas for wavelengths of 0.7 μ, we use cylinders 100 μ in length and 10 μ in radius because a large amount of computer time will be wasted otherwise. Mie computations for spheres [*Liou and Hansen*, 1971] are also made for the comparisons in phase functions. The modified gamma functions for particle size distributions [*Deirmendjian*, 1969] of clouds enter primarily in smoothing the rapid oscillations of phase functions due to single-particle effects. Otherwise, mean values of particle size are used. No attempt is made here to discuss the effect of size distributions of clouds on the scattered radiation.

Figure 1 illustrates the normalized phase functions for the four cases denoted above. At λ = 0.7, 2, and 2.5 μ the noticeable broad maximums around 135° for cylinders are similar to the first cloud bows produced by the scattering of spheres, as we can see in the figures. These features arise from rays incident normally or near normally on the cylinders. The glory that is caused by the backscattering of edge rays from spheres, however, disappears in the case of scattering by ice cylinders. At λ = 3 μ, because of the large absorption involved, no

TABLE 1. Optical Properties for Randomly Oriented Ice Cylinders

λ, μ	n_r	n_i	l, μ	r, μ	$\tilde{\omega}_0$	$\langle\cos\Theta\rangle$	β_e, km^{-1}
0.7	1.310	0.0	100	10	1.0	0.735	1.902
2.0	1.291	1.61×10^{-3}	200	30	0.783	0.750	12.801
2.5	1.235	7.95×10^{-4}	200	30	0.901	0.753	13.570
3.0	1.130	0.2273	200	30	0.524	0.651	12.585

Particle number density is 0.5 cm^{-3}, l is length, and r is radius.

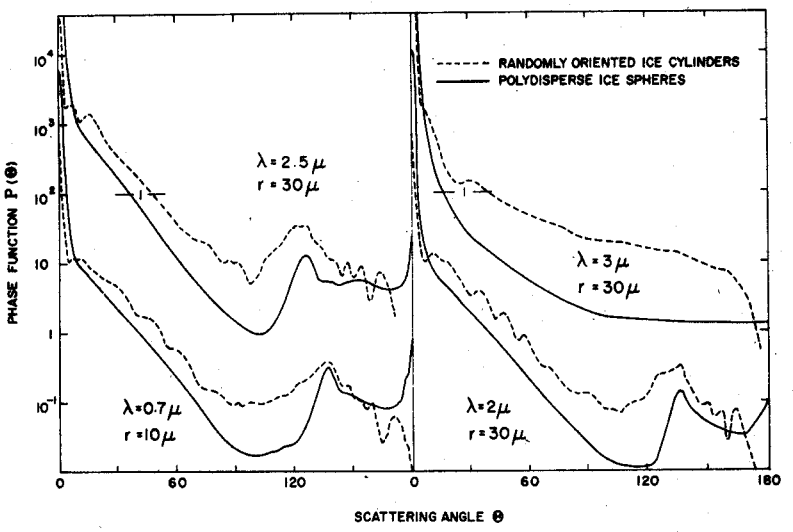

Fig. 1. Phase functions for randomly oriented ice cylinders (dashed lines) and ice spheres (solid lines) at incident wavelengths of 0.7, 2, 2.5, and 3 μ. The vertical scale applies to the lower curves; the upper curves are displaced upward by factors of 10^2.

features are produced. It is probable that for more irregular crystals the maximums similar to cloud bows would also disappear. In general, cylinders seem to scatter more light in regions from ~20° to ~160° at the expense of both the forward and the backward scattering.

In addition to the phase functions some single-scattering properties of the randomly oriented cylinders are also given in Table 1. Here n_r and n_i are the real and imaginary parts of the refractive indices for ice, respectively. The asymmetry factor $\langle \cos \Theta \rangle$ is a quantity describing the degree of forward scattering of the phase function (see next section for the mathematical definition). Moreover, we have assumed an averaged number density of 0.5 cm^{-3} for ice cylinders in cirrus so that the volume extinction cross section β_e could be evaluated. Because of the small sizes used in the case of the visible wavelength, it should be noted that the volume extinction cross section is about a factor of 6 smaller than the volume extinction cross sections of the rest of the cases.

Modified Two-Stream Approximation for Radiative Transfer

Theoretical developments. Since we are primarily interested in the vertical distribution of fluxes in this study, we consider that radiation fields preserve with axial symmetry. The appropriate equation describing the diffuse radiation field is therefore

$$\mu \frac{dI(\tau, \mu)}{d\tau} = -I(\tau, \mu) + \frac{1}{2}\int_{-1}^{+1} P(\mu; \mu')I(\tau, \mu')\, d\mu' + \frac{1}{4} F_0 P(\mu; \mu_0) \exp(-\tau/\mu_0) \qquad (14)$$

where the notation I denotes intensity, τ is the optical thickness, F_0 is the incident solar flux, $\mu = \cos\theta$, θ is the emergent angle, $\mu' = \cos\theta'$, θ' is the incident angle, $\mu_0 = \cos\theta_0$, and θ_0 is the zenith angle. The phase function P can be expanded in Legendre polynomials consisting of a finite number of terms [*Chandrasekhar*, 1950]:

$$P(\cos\Theta) = \sum_{l=0}^{N} \tilde{\omega}_l p_l(\cos\Theta) \qquad (15)$$

where Θ represents the angle between the incident wave and the scattered wave (i.e., the scattering angle) and $\tilde{\omega}_l (l = 0, 1, \cdots, N)$ are a set of $N + 1$ constants that can be determined by

$$\tilde{\omega}_l = \frac{2l+1}{2} \cdot \int_{-1}^{+1} P(\cos\Theta) p_l(\cos\Theta)\, d\cos\Theta \qquad (16)$$

In (16), $\tilde{\omega}_0$ denotes the well-known single-scattering albedo, and $\tilde{\omega}_1/3\tilde{\omega}_0$ (usually denoted as g or $\langle\cos\Theta\rangle$) represents the asymmetry factor, which describes the degree of the forward scattering of phase function. By means of the addition theorem of spherical harmonics, assuming azimuth independence, we have expansion of phase function of

$$P(\mu;\mu') = \sum_{l=0}^{N} \tilde{\omega}_l p_l(\mu) p_l(\mu') \qquad (17)$$

Define the downward and upward fluxes that are normal to the plane-parallel layer as follows:

$$F(\tau) = 2\pi \int_0^{\pm 1} I(\tau,\mu)\mu\, d\mu \qquad (18)$$

where $\mu > 0$ for $F\downarrow(\tau)$ and $\mu < 0$ for $F\uparrow(\tau)$. In MTSA, two approximations are made. First, we define a constant in the left-hand side of (14) as

$$\langle\mu\rangle = \int_0^1 I(\tau,\mu)\mu^2\, d\mu \Big/ \int_0^1 I(\tau,\mu)\mu\, d\mu \qquad (19)$$

This constant may be determined from the conservation of energy and is discussed at the end of this section. In view of the polynomial form of phase function the intensity may also be expressed as

$$I(\tau,\mu) = \sum_{k=0}^{N} I_k(\tau) p_k(\mu) \qquad (20)$$

where p_k again is the Legendre polynomial of order k. If the above expression is employed and the orthogonal properties of the Legendre polynomials are noted, the second term in the right-hand side of (14) becomes

$$\int_{-1}^{+1} P(\mu;\mu') I(\tau,\mu')\, d\mu' = \sum_{l=0}^{N} \frac{2}{2l+1} \tilde{\omega}_l p_l(\mu) I_l(\tau) \qquad (21)$$

The second approximation is made by taking two terms in (20) and (21), i.e., $N = 1$.

On the basis of the above two assumptions, two equations for the downward and upward fluxes can be derived:

$$\langle\mu\rangle \frac{dF\downarrow(\tau)}{d\tau} = -F\downarrow(\tau) + F\downarrow(\tau)\tilde{\omega}_0(1-b) + F\uparrow(\tau)\tilde{\omega}_0 b + q\downarrow \exp(-\tau/\mu_0) \qquad (22)$$

and

$$-\langle\mu\rangle \frac{dF\uparrow(\tau)}{d\tau} = -F\uparrow(\tau) + F\uparrow(\tau)\tilde{\omega}_0(1-b) + F\downarrow(\tau)\tilde{\omega}_0 b + q\uparrow \exp(-\tau/\mu_0) \qquad (23)$$

where

$$b = (1 - \langle\cos\Theta\rangle)/2 \qquad (24)$$

and

$$q = \pi\mu_0 F_0 \frac{1}{2\mu_0} \sum_{l=0}^{N} \tilde{\omega}_l p_l(\mu_0) \int_0^{\pm 1} p_l(\mu)\mu\, d\mu \qquad (25)$$

In (25), $\mu > 0$ for $q\downarrow$, $\mu < 0$ for $q\uparrow$, and $\pi\mu_0 F_0$ represents the solar flux incident perpendicularly to the plane-parallel layers. The quantity b in (24) indicates the fraction of radiation singly scattered in the backward hemisphere. It should be noted that the direct solar radiation term remains without further assumption. This may physically be explained as treating the single scattering exactly.

Equations 22 and 23 represent two first-order nonhomogeneous differential equations. The standard derivations for such systems yield the following simultaneous solutions:

$$F\downarrow(\tau) = v\exp(c\tau)K + u\cdot\exp(-c\tau)H + \epsilon\exp(-\tau/\mu_0) \qquad (26)$$

$$F\uparrow(\tau) = u\exp(c\tau)K + v\cdot\exp(-c\tau)H + \gamma\exp(-\tau/\mu_0)$$

where

$$v = (1-a)/2 \qquad u = (1+a)/2$$
$$\epsilon = (\alpha+\beta)/2 \qquad \gamma = (\alpha-\beta)/2$$
$$c^2 = (1-\tilde{\omega}_0)(1-\tilde{\omega}_0 g)/\langle\mu\rangle^2$$
$$a^2 = (1-\tilde{\omega}_0)/(1-\tilde{\omega}_0 g)$$

$$\alpha = \frac{\pi\mu_0 F_0[(1-\tilde{\omega}_0 g)\mu_0^2(q\downarrow + q\uparrow) + \mu_0\langle\mu\rangle(q\downarrow - q\uparrow)]}{\langle\mu\rangle^2(c^2\mu_0^2 - 1)}$$

$$\beta = \frac{\pi\mu_0 F_0[(1-\tilde{\omega}_0)\mu_0^2(q\downarrow - q\uparrow) + \mu_0\langle\mu\rangle(q\downarrow + q\uparrow)]}{\langle\mu\rangle^2(c^2\mu_0^2 - 1)}$$

The constants K and H have to be determined by the following boundary conditions for the diffuse fluxes at the top and bottom of the scattering layer:

$$F\downarrow(0) = 0$$
$$F\uparrow(\tau_n) = A_s[F\downarrow(\tau_n) + \pi\mu_0 F_0 \exp(-\tau_n/\mu_0)] \quad (27)$$

i.e., there is no diffuse flux at the top of the layer, and the underlying surface with albedo A_s reflects the total downward flux (diffuse plus direct) at level τ_n.

Substituting the above two conditions into (26) and solving for K and H, we obtain the two constants as follows:

$$K = \frac{-\{\epsilon(v - uA_s)\exp(-c\tau_n) + [(1+\epsilon)A_s - \gamma]u\exp(-\tau_n/\mu_0)\}}{v(v - A_s\mu)\exp(-c\tau_n) - u(u - A_s v)\exp(c\tau_n)}$$
$$H = \frac{\{\epsilon(u - vA_s)\exp(c\tau_n) + [(1+\epsilon)A_s - \gamma]v\exp(-\tau_n/\mu_0)\}}{v(v - A_s u)\exp(-c\tau_n) - u(u - A_s v)\exp(c\tau_n)} \quad (28)$$

Hence the solutions for the upward and downward diffuse fluxes are complete. The radiation field on the boundary, i.e., the diffuse reflection and transmission for a cloud layer, can easily be obtained from (26):

$$r = \frac{F\uparrow(0)}{\pi\mu_0 F_0} = \frac{1}{\pi\mu_0 F_0}(uK + vH + \gamma)$$
$$t = \frac{F\downarrow(\tau_n)}{\pi\mu_0 F_0} = \frac{1}{\pi\mu_0 F_0}[v\exp(c\tau_n)K + u\exp(-c\tau_n)H + \epsilon\exp(-\tau_n/\mu_0)] \quad (29)$$

From the law of the conservation of energy, if A_s equals 0 and $\tilde{\omega}_0$ approaches 1, the sum of the total transmission and reflection should also approach 1. Thus, after making some algebraic operations, we obtain the constant defined in (19) as follows:

$$\langle\mu\rangle \simeq \mu_0(q\downarrow + q\uparrow) \quad (30)$$

Finally, it should be noted that all the above discussions were for nonconservative scattering. For conservative scattering a set of simpler equations similar to those described above can be derived, since $\tilde{\omega}_0 = 1$ implies singularity in (28). However, using $\tilde{\omega}_0 = 0.99999$, we found that the results are practically the same as those of conservative scattering with an accuracy up to at least three decimal points. Consequently, for all practical purposes there is no need to present additional formulas for conservative scattering.

Comparisons with doubling method. To examine the accuracy of MTSA, we made several comparisons with the more exact transfer computations by means of a doubling method. The doubling method has been very successfully developed in the last few years [*Hovenier*, 1971; *Hansen*, 1971] since *van de Hulst* [1963] outlined the general numerical procedures for it. In the comparisons discussed below, the phase functions employed in the calculations of MTSA are exactly the same as those used in doubling computations.

Figure 2 compares the reflection (or local albedo) evaluated by MTSA with that of doubling computations previously reported by *Hansen* [1969, Figure 3]. The left- and right-hand sides are results for a water cloud and a haze, respectively, when the modified gamma function for the size distributions [*Deirmendjian*, 1969] illuminated by a wavelength of 0.8189 μ was used. Both cases are for conservative scattering with asymmetry factors of 0.844 for the cloud and 0.794 for the haze. The comparisons show a fair agreement between the two methods. The error produced due to the approximation is less than 3% in all cases except in near-grazing angles for a small optical thickness of 0.5.

Figure 3 shows some comparisons of the two methods for the reflection as a function of the optical thickness when the sun is illuminating normally to the plane-parallel layer. The doubling computations were published by *Irvine* [1968, Figure 5] employing the phase function for water spheres having size parameters of 20. Three cases of single-scattering albedo, 1, 0.984, and 0.8, were shown. The results again reveal

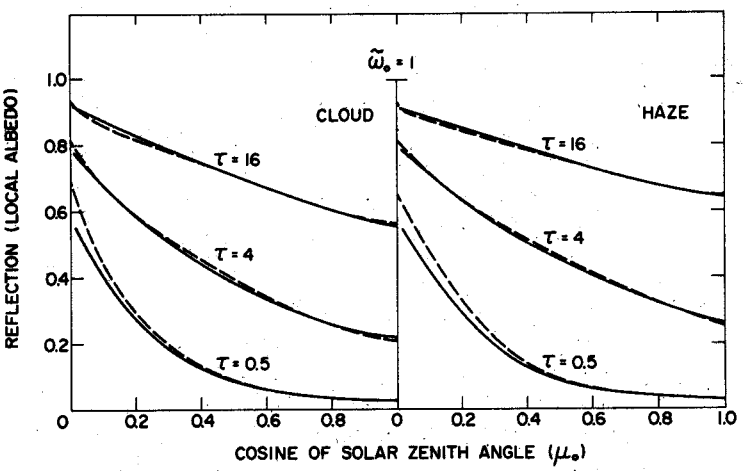

Fig. 2. Comparisons of the reflection calculations between MTSA (solid lines) and the doubling method (dashed lines) published by *Hansen* [1969]. The left- and right-hand sides are results for a water cloud and a haze, respectively. Both cases are for conservative scattering.

in general a good agreement between the two methods. In the second case, where the absorption is small, it appears that the error due to approximation becomes greater for larger optical thickness.

Although the second comparison includes cases of absorption, all the results are only for normal incidence. We have not been able to locate the detailed values of reflection and transmission for large and small absorption in the literature. J. E. Hansen (unpublished data, 1972) has kindly provided me with some of his material, so that a comprehensive comparison illustrated in Figure 4 was made possible. In this figure, two cases were displayed for both diffuse transmission and reflection as functions of zenith angle. The phase functions employed were computed for water spheres by using a gamma function for size distribution with a mean radius of 10. The upper graphs are for the incident wavelength of 3 μ, where large absorption occurs and the scattering concentrates mainly on the forward direction (g = 0.940). It is seen that the differences between the values obtained by MTSA and the doubling method are practically insignificant. The lower graphs denote the case for an incident wavelength of 2.5 μ, where the absorption is quite small. For τ = 16 some differences ($\sim$7%) were found at near-normal incidence for both diffuse transmission and reflection. However, for τ = 0.5 and 4, the comparisons between the two methods appear to be quite satisfactory with an accuracy of $\sim$3%.

After these comprehensive comparisons with the doubling computations we conclude that the modified two-stream approximation for radiative transfer is an excellent approximating

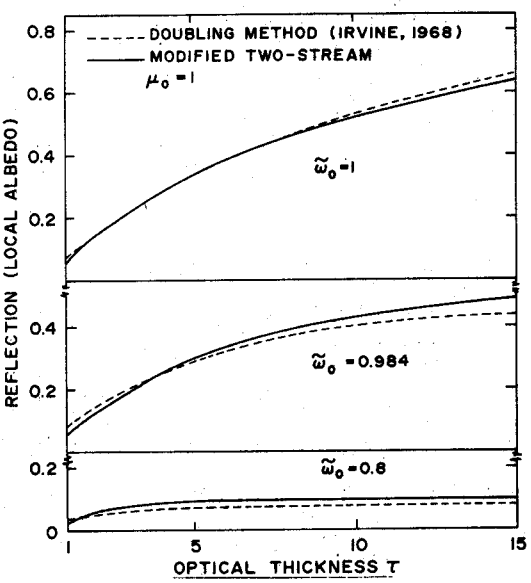

Fig. 3. Comparisons of the reflection computations between MTSA (solid lines) and the doubling method (dashed lines) reported by *Irvine* [1968] for normal incidence. Two absorption cases are shown.

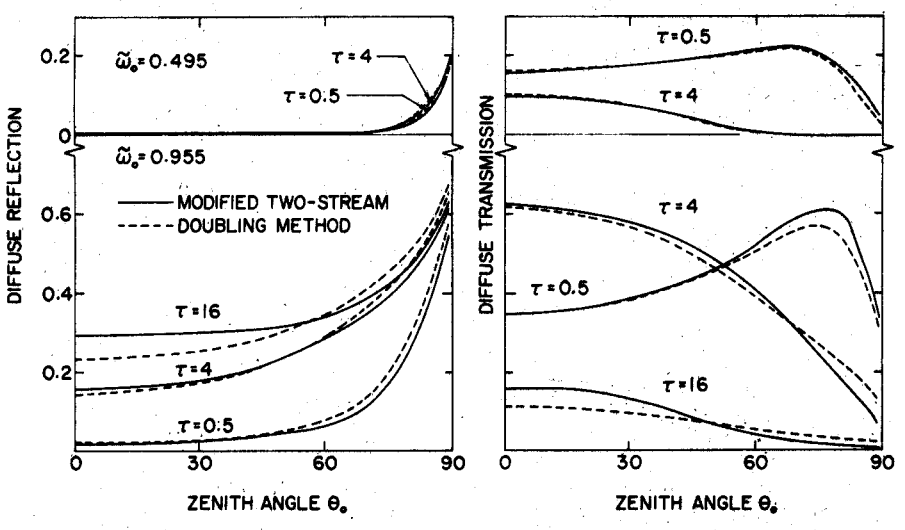

Fig. 4. Comparisons of the reflection and diffuse transmission for cases of small and large absorption evaluated by MTSA (solid lines) and those by the doubling method (dashed lines) kindly provided by J. E. Hansen.

method. It involves only a very small amount of computer time because the analytic solutions can be explicitly derived. Moreover, the method provides an easier means to evaluate the flux distribution in the scattering layer.

RESULTS AND DISCUSSIONS

In the section on single scattering by randomly oriented ice cylinders, results of single-scattering computations for the hypothetical cirrus cloud models were described, and thus optical properties of such models may be put into the approximated radiative transfer program discussed in the preceding section. Three wavelengths, 0.7, 2.5, and 3 μ, were chosen in radiation computations because at these wavelengths of the solar spectrum ice particles possess properties of no, small, and large absorption accordingly. The phase functions of ice cylinders were expanded into the form of Legendre polynomials. They normally take about 20 significant terms, which were used to evaluate (25). Transmission and reflection are presented as functions of zenith angle as well as the geometric thickness of cirrus. The geometric thickness can easily be converted into

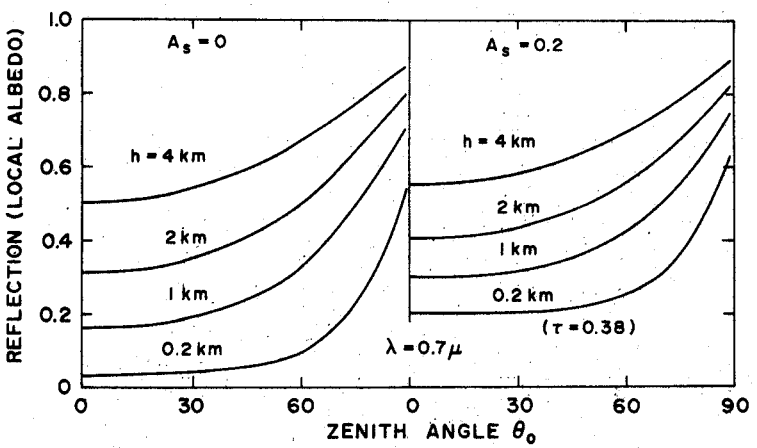

Fig. 5. Reflection as a function of zenith angle for several geometric thicknesses of cirrus illuminated by a visible wavelength of 0.7 μ. Underlying surface albedoes of 0 and 0.2 are used.

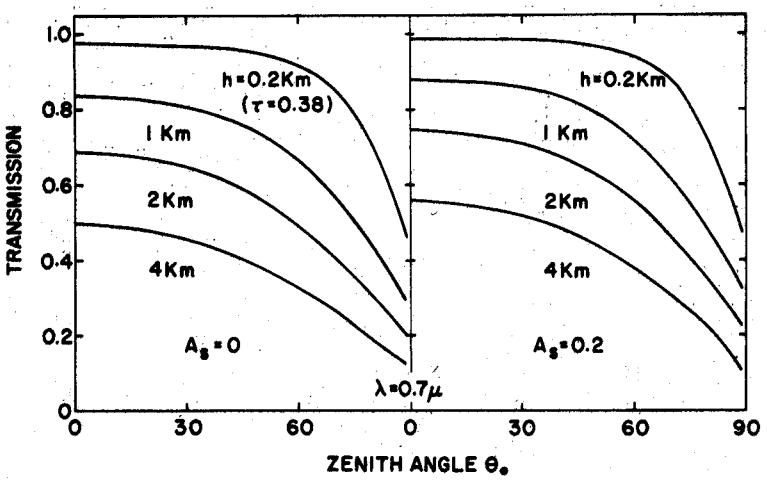

Fig. 6. Transmission as a function of zenith angle for several geometric thicknesses of cirrus illuminated by 0.7 μ visible light.

the optical thickness. (Basic values are shown in each figure.) It should be noted that a particle concentration of 0.5 cm^{-3} was used throughout the calculations.

Figures 5 and 6 illustrate reflection (or local albedo) and total transmission (diffuse plus direct) as functions of the solar zenith angle at the 0.7 μ visible wavelength. The direct transmission of solar radiation is simply equal to exp $(-\tau/\mu_0)$. The left- and right-hand sides of both figures are for underlying surface albedoes of 0 and 0.2, respectively. We have used thicknesses of 0.2, 1, 2, and 4 km for the cirrus cloud layers. They correspond to the optical thicknesses of ~0.4, 2, 4, and 8, respectively. For a typical cirrus with an optical thickness of ~2 the albedo is ~20% up to the zenith angle of ~60°. The underlying surface of cirrus (such as other clouds, aerosols, or ground) appears to provide the additional upward fluxes that apparently increase the albedo of cirrus, particularly for thin cirrus because it usually

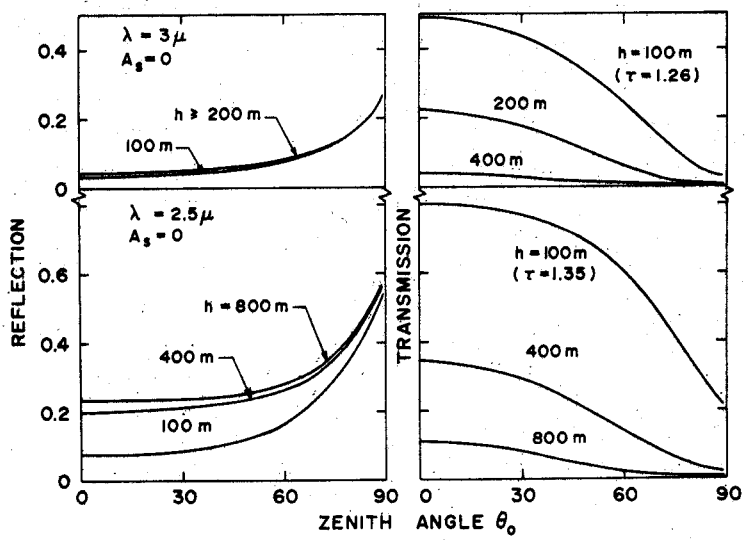

Fig. 7. Reflection and transmission as functions of zenith angle for cirrus cloud layers illuminated by two near-infrared wavelengths of 2.5 and 3 μ.

has large values of transmission. The large transmission of thin cirrus can often be observed in nature, since we can see when sunlight penetrates it. The values of transmission can be as high as 90% for most zenith angles. Even for thick cirrus having an optical thickness of ~4, ~60% transmission for most zenith angles is seen in our results.

Figure 7 shows values of transmission and reflection for the two near-infrared wavelengths. At $\lambda = 3\ \mu$, owing to the large amount of absorption, small values of reflection that tend to saturate at an optical thickness of $\gtrsim 2$ are obtained. On the other hand, despite the large absorption involved, transmission can still be quite large because the unscattered component of radiation dominates. At $\lambda = 2.5\ \mu$, where the absorption is small, values of reflection are unchanged when the optical thickness reaches ~10 and little light is transmitted. Finally, the values of absorption may be obtained by subtracting the total sum of transmission and reflection from the incident solar flux, which is normalized to be 1. The amounts of absorption are hence responsible for the heating effect in the cirrus.

Acknowledgments. I wish to thank Professor R. G. Fleagle for reading the manuscript. This research was supported by the National Science Foundation under grant GU-2655. Portions of the computations were performed while I held a NRC research associateship supported by Goddard Institute for Space Studies, NASA. Contribution 271, Department of Atmospheric Sciences, University of Washington, Seattle, Washington 98195.

REFERENCES

Chandrasekhar, S., *Radiative Transfer,* 393 pp., Dover, New York, 1950.

Cox, S. K., Cirrus cloud and the climate, *J. Atmos. Sci., 28,* 1513–1515, 1971.

Deirmendjian, D., *Electromagnetic Scattering on Spherical Polydispersions,* 290 pp., Elsevier, New York, 1969.

Fritz, S., and P. K. Rao, On the infrared transmission through cirrus clouds and the estimation of relative humidity from satellites, *J. Appl. Meteorol., 6,* 1088–1096, 1967.

Hall, F. F., A physical model of cirrus 8–13 μ infrared radiance, *Appl. Opt., 7,* 2264–2269, 1968.

Hansen, J. E., Exact and approximate solutions for multiple scattering by cloudy and hazy planetary atmospheres, *J. Atmos. Sci., 26,* 478–487, 1969.

Hansen, J. E., Multiple scattering of polarized light in planetary atmospheres, 2, Sunlight reflected by terrestrial water clouds, *J. Atmos. Sci., 28,* 1400–1426, 1971.

Hovenier, J. W., Multiple scattering of polarized light in planetary atmospheres, *Astron. Astrophys., 13,* 7–29, 1971.

Irvine, W. M., Multiple scattering by large particles, 2, Optically thick layers, *Astrophys. J., 152,* 828–834, 1968.

Irvine, W. M., and J. B. Pollack, Infrared optical properties of water and ice spheres, *Icarus, 8,* 324–366, 1968.

Kerker, M., *The Scattering of Light and Other Electromagnetic Radiation,* 666 pp., Academic, New York, 1969.

Kuhn, P. H., and H. K. Weickmann, High altitude radiometric measurements of cirrus, *J. Appl. Meteorol., 8,* 147–154, 1969.

Liou, K. N., Electromagnetic scattering by arbitrarily oriented ice cylinders, *Appl. Opt., 11,* 667–674, 1972*a*.

Liou, K. N., Light scattering by ice clouds in the visible and infrared: A theoretical study, *J. Atmos. Sci., 29,* 524–536, 1972*b*.

Liou, K. N., and J. E. Hansen, Intensity and polarization for single scattering by polydisperse spheres: A comparison of ray-optics and Mie theory, *J. Atmos. Sci., 28,* 995–1004, 1971.

McElroy, M. B., The composition of planetary atmosphere, *J. Quant. Spectrosc. Radiat. Transfer, 11,* 813–825, 1971.

Shettle, E. P., and J. A. Weinman, The transfer of solar irradiance through inhomogeneous turbid atmosphere evaluated by Eddington's approximation, *J. Atmos. Sci., 27,* 1048–1055, 1970.

Twersky, V., Certain transmission and reflection theorem, *J. Appl. Phys., 25,* 859–862, 1954.

van de Hulst, H. C., *Light Scattering by Small Particles,* 470 pp., Wiley, New York, 1957.

van de Hulst, H. C., A new look at multiple scattering, *NASA Tech. Rep.,* 81 pp., 1963.

Weickmann, H. K., Die Eisphase in der Atmosphere, 54 pp., *Ber. Deut. Wetterdienstes U.S. Zone,* no. 6, 1949.

(Received October 17, 1972.)